Journal of Applied Polymer Science

Thermoelectric Performance of Electrodeposited Nanostructured Polyaniline Doped with Sulfo-Salicylic Acid

Krishanu Chatterjee,[1] Mousumi Mitra,[1] Saibal Ganguly,[2] Kajari Kargupta,[3] Dipali Banerjee[1]

[1]Department of Physics, Bengal Engineering and Science University, Howrah 711103, India

[2]Department of Chemical Engineering, Universiti Teknologi Petronas, Malaysia

[3]Department of Chemical Engineering, Jadavpur University, Kolkata 700032, India

Correspondence to: D. Banerjee (E-mail: dipalibanerjeebesu@gmail.com or banerjee_dipali@yahoo.co.in)

ABSTRACT: Conducting polymers, in present days, are considered to be potential thermoelectric (TE) materials. Among them polyaniline (PANI) is a promising candidate. Nanostructured polyaniline doped with organic dopant is electrodeposited and structurally characterized. Its transport properties are investigated for thermoelectric applications. The analysis of transmission electron microscopy image reveals that the sample is rod like nanostructure. This study shows that the type (inorganic/organic) of dopants plays an important role to influence the dimension of nanostructure and the electrical transport properties of PANI. In this study, organic dopant sulfosalicylic acid is proposed for enhancement of figure of merit through an increase in thermoelectric power and decrease in thermal conductivity. Compared to our earlier work the figure of merit evaluated is two orders higher than that of the inorganic dopant bismuth nitrate doped PANI. © 2013 Wiley Periodicals, Inc. J. Appl. Polym. Sci. **2014**, *131*, 39920.

KEYWORDS: nanostructured polymers; films; properties and characterization

Received 3 July 2013; accepted 1 September 2013

DOI: 10.1002/app.39920

INTRODUCTION

The discovery of conducting polymers (CP) directs a new trend of research. Since the discovery in early seventies, these polymers have made a significant impact and provided a vast field for a number of growing new technologies.[1–4] The importance of environmental protection is well understood which led to focus in the development of suitable thermoelectric (TE) conducting polymer based material. They are thought to be potential thermoelectric materials due to their high value of electrical conductivity to thermal conductivity ratio compared to that of inorganic materials.[5–7] The transport properties of these conducting polymers are greatly influenced by the nature of dopants. Out of the CPs, polyaniline (PANI)[8] gained its importance as a potential candidate to be used as TE material due to its high environmental stability, ease of processing,[9] simple and reversible doping/dedoping chemistry,[10] and modifiable electrical conductivity.[11] For the enhancement of transport properties, different protonic acids have been used to dope PANI. Typical examples of some organic and inorganic acids used as dopants are HCl, H_2SO_4, $HClO_4$[12–14] *p*-toluenesulfonic acid, benzenesulfonic,[15] *p*-styrenesulfonic acid,[16] polyacrylic acid,[17] and sulfosalicylic acid.[18,19] Doped nanostructured PANI shows better performance as thermoelectric material.[20]

In an earlier work, we have reported the power factor of bismuth nitrate doped PANI but ZT could not be measured due to lack of facility. In this study, PANI films has been electrodeposited using sulfosalicylic acid as organic dopant and bismuth nitrate as inorganic dopant[20] to investigate and compare the enhancement in power factor and figure of merit in the two cases. The film was structurally characterized to map with the properties. Comparing with the reported values,[20] it is observed that the power factors at and near room temperatures are enhanced by the use of the organic dopant. Due to low value of thermal conductivity for SSA-doped PANI the figure of merit is found to be two order more than bismuth nitrate doped PANI. Doping mechanism for the two cases has been described to explain the above observation.

EXPERIMENTAL

Materials

Emeraldine base was purchased from Alfa Aesar. Sulfo-salicylic acid (SSA) and *N*,*N*-dimethyl formamide (DMF) were purchased from Emerck. ITO coated glass was purchased from SPI supplies. All other chemicals were of analytical reagent grade and are used without further purification.

Solution Preparation

About 2 mg mL^{-1} PANI emeraldine base was dissolved in DMF and kept under soft ultra sonication with a piezo-u-sonic ultrasonic processor for about 2 h. SSA was mixed to the above

solution as dopant and the resulting solution was again sonicated for a few minutes. Green colored solution was obtained immediately after the addition of the organic dopant.

Electrochemical Deposition

As described in our earlier work,[21] an electrochemical cell of 50 mL of volume was covered with a wooden support having provisions to hold Indium Tin Oxide (ITO) coated glass as cathode, graphite as anode and a hole for saturated calomel electrode as reference electrode. Prior to use ITO was washed with distilled water and ethanol to ensure the removal of any impurity. A dc voltage of 20 V was applied to the solution through the electrodes and the depositions were carried out. Thin film of doped PANI was deposited on ITO coated glass which was dried in a vacuum oven for 1 h.

Characterization

For the structural characterization, Fourier transform infrared (FTIR) spectrum of the prepared sample was conducted by a Shimadzu Spectrophotometer. The FTIR spectrum was taken in the range 500–3500 cm^{-1}. Transmission electron microscopy image was obtained by Technai transmission electron microscope at a typical accelerating voltage of 200 kV to understand the structural morphology of electrodeposited thin film of PANI. The measurements of electrical conductivity (σ) as well as thermoelectric power (S) were carried out in the temperature range 290–400 K. The electrical conductivity was calculated from the following formula:

$$\text{Conductivity}\ (\sigma) = l/Rbt \qquad (1)$$

where l is the length of the film, R is the resistance of the film which is calculated from the $I-V$ characteristics of the samples, b is the breadth of the film, and t is the thickness of the film. For the measurement of thermoelectric power, an auxiliary heater placed at one end of the sample holder, creates a temperature difference, while the corresponding potential drop was measured by a Hewlett Packard data acquisition system (Model No. 34970A). The thermal conductivity measurements at room-temperature were carried out for the prepared samples using a Hot Disk thermal constants analyzer (TPS 2500 S, Sweden).

RESULTS AND DISCUSSION

Structural Characterization

Fourier Transform Infrared Analysis. Figure 1 shows the Fourier transform infrared (FTIR) spectra in the range 500–3500 cm^{-1} of the SSA-doped PANI. The spectra show strong bands between 600–1800 cm^{-1}, which are the characteristics of PANI. The peak at 817 cm^{-1} was assigned to the aromatic C–H bending out of the plane for 1,4-di-substituted benzene ring.[22] The peaks at 1146 and 1301 cm^{-1} represents in-plane C–H bending of quinoid structure and C–N stretching of secondary aromatic amine respectively.[23] The peaks at 1490 and 1575 cm^{-1} represents C=N stretching of the quinoid and C=C stretching of the benzoid rings.[24]

The characteristics bands observed at 592 and 667 cm^{-1} are attributed to out-of-plane bending of SSA ring and in-plane bending and/or out-of-plane bending of SSA ring, respectively. The distinctive bands at 804 and 883 cm^{-1}, corresponding to γ C–H vibration of SSA ring and ~1025 cm^{-1}, attributed to symmetric stretching of SO_3 group, confirm that PANI-SSA samples are doped with 5-sulfosalicylate anions.[25–27] Further the characteristic band observed at 1666–1678 cm^{-1} signifies the C=O stretching of COOH confirming the presence of SSA as dopant in PANI.

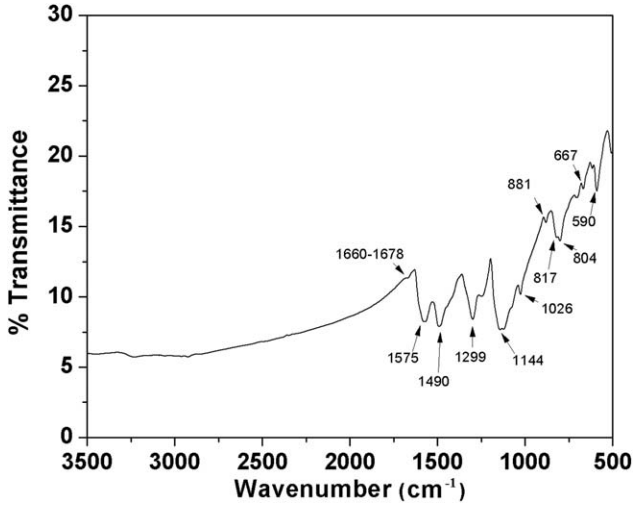

Figure 1. FTIR spectrum of SSA-doped electrodeposited PANI.

Transmission Electron Microscopic Analysis. Image of transmission electron microscope of SSA-doped PANI is shown in Figure 2(a). The prepared sample show long nanorods like structures as obtained in the case of bismuth nitrate doped PANI.[20] It is worth mentioning that irrespective of the type of dopants, both the samples synthesized by the method of electro-deposition exhibit nanorod like structures but have different dimensions tabulated in Table I.

Scanning Electron Microscopic Analysis. The cross-section SEM image of the film is shown in Figure 2(b). The average thickness of the sample as observed from the figure (2.2×10^{-3} cm) is of the same order as found gravimetrically (3×10^{-3} cm).

Electrical Characterization

Electrical Conductivity. The emaraldine base (EB) form of PANI recognized as an insulator can be converted to conductor or semiconductor by the process of doping. Various reports show that PANI can be doped with both organic and inorganic dopants[5,11,28–30] and the electrical conductivity (σ) of PANI greatly depends on the nature of dopants. In our exploration, it was observed that σ of PANI changes with the nature of dopants. The room temperature value of σ for SSA-doped PANI (74.07 S cm^{-1}) is found to be about five times more than that of the value of bismuth nitrate doped PANI (15.09 S cm^{-1}) as reported in literature[20] and much less than HCl doped PANI.[31] The temperature dependence of σ of the electrodeposited sample has been shown in Figure 3(a). Though the sample show a metallic type of conduction but the variation is non-linear. For the explanation of electrical properties of conducting polymers,

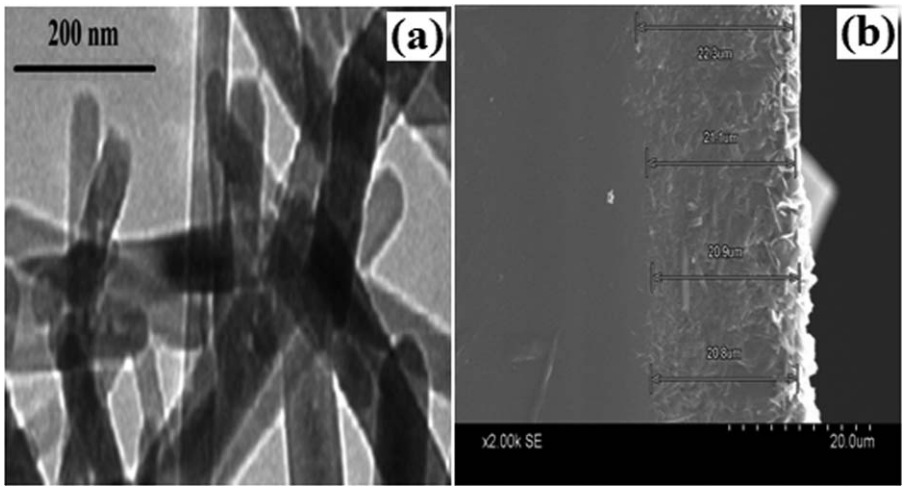

Figure 2. (a) TEM image of SSA-doped electrodeposited PANI showing nanorod like structures. (b) Cross-section SEM image of the prepared thin film.

Table I. Different Parameters of Organic and Inorganic Doped PANI at Room Temperature: A Comparison

Dopants	Size from TEM	σ (S cm^{-1})	S (μV K^{-1})	P (μW m K^{-2})	κ (W m^{-1} K^{-1})	ZT	Remarks
SSA	Average diameter and length of 50 nm and 370 nm respectively	74.07	−11.37	0.95761	0.1869	1.56×10^{-3}	This study
$Bi(NO_3)_3$	Average diameter and length of 25 nm and 250 nm respectively	15.09	−3.72	0.06224	0.7130	2.62×10^{-5}	Ref. 20

quite a few mechanisms have been put forward. Long et al.,[11] Kaiser et al.,[32,33] Park et al.[34], and Holland et al.[35] proposed that the charge transport is associated with a metallic conduction within the metal islands with a hopping or tunneling effect due to the insulating barriers. This decreases the value of σ in both the samples. Conduction in polymer is caused by the hopping of polarons from one site to another along the chain. To explain the temperature variation of conductivity with temperature, Kaiser et al.[33] put forward a quasi one-dimensional metallic contribution with fluctuation induced tunneling between the extended metallic islands within an amorphous matrix to obtain an expression

$$\sigma^{-1} = \rho_m \exp\left(\frac{-T_m}{T}\right) + \rho_t \exp\left(\frac{T_C}{T+T_S}\right) \quad (2)$$

where ρ_m, ρ_t, T_m are constants and T_c and T_s are Sheng parameters which depend on the tunneling process. Considering the present case, we observe that there is a non linear decrease of σ with T for the sample suggesting that the conduction is metallic type with a tunneling mechanism functioning for the carriers between the nanorods that are produced at the time of deposition. Decrease in conductivity at higher temperature is due to the complete delocalization of charge carriers[35] as has also been observed for HCl doped PANI.[31]

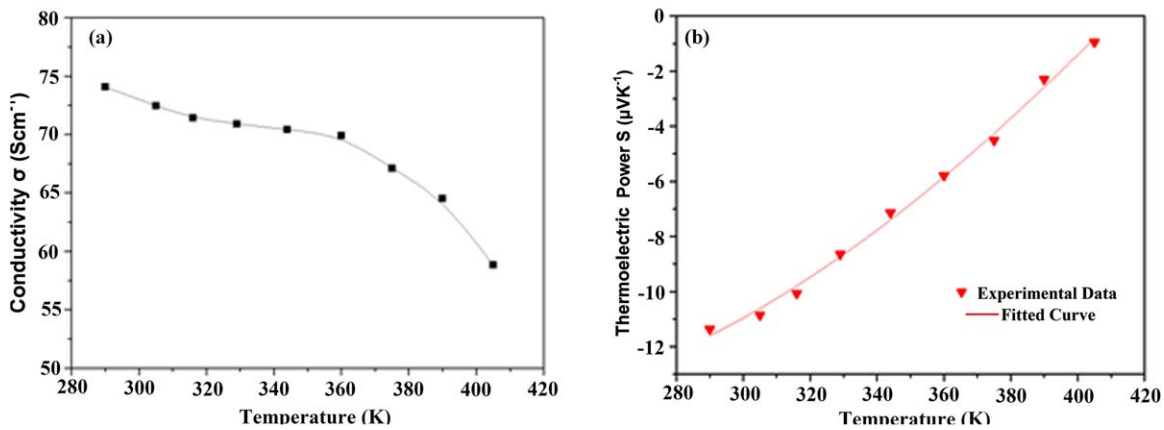

Figure 3. Variation of (a) electrical conductivity and (b) thermoelectric power of SSA-doped electrodeposited PANI with temperature. [Color figure can be viewed in the online issue, which is available at wileyonlinelibrary.com.]

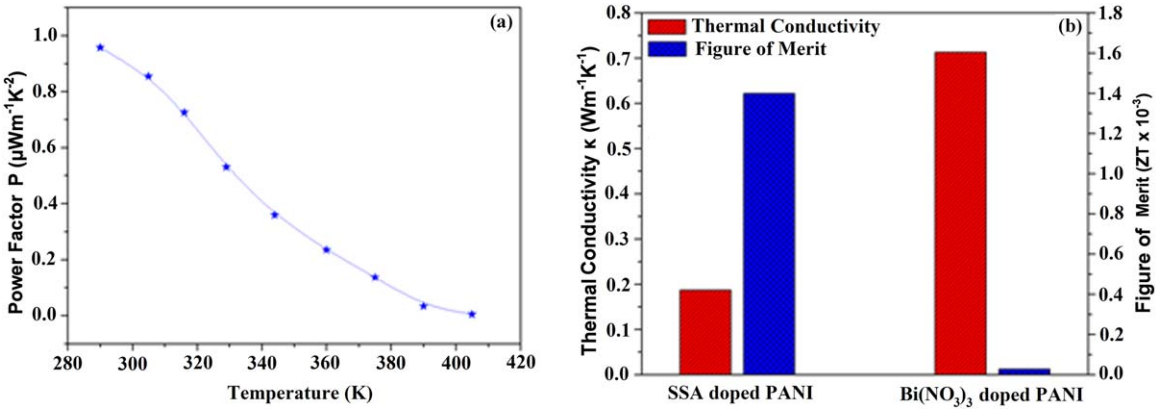

Figure 4. (a) Variation of power factor with temperature of SSA-doped PANI and (b) thermal conductivity and figure of merit of SSA and $Bi(NO_3)_3$ doped electrodeposited PANI at room temperature. [Color figure can be viewed in the online issue, which is available at wileyonlinelibrary.com.]

Thermoelectric Power (S). The values of *S* of the electrodeposited films of nanostructured PANI have been measured and the temperature variation is shown in Figure 3(b). It is observed that electrons are the majority carriers as confirmed from the negative values of *S* at room temperature. The negative value of *S* decreases with the increase in temperature with a tendency of becoming positive at higher temperature as was observed in bismuth nitrate doped PANI.[20] The *S* value at room temperature for SSA-doped PANI (-11.37 μV K^{-1}) is found to be more than that of bismuth nitrate doped PANI (-3.72 μV K^{-1}).[20]

Monkman and co-workers[35] proposed a composite model taking into account the metallic contribution to *S* due to intrachain transport and the effect of interchain hopping. Considering these two effects the present experimental data of *S* is fitted well with the equation given by

$$S = A + BT - CT^{1/2} \quad (3)$$

where *A*, *B*, and *C* are fitting parameters. The second term contributes to the metallic thermoelectric power and the third term is the characteristics of the hopping mechanism.

Power Factor (P). Figure 4(a) shows the temperature variation of the power factor ($P = S^2\sigma$) of SSA-doped PANI. Room temperature values of conductivity and thermoelectric power of SSA-doped PANI being higher than that of bismuth nitrate doped PANI,[20] the power factor at room temperature is greater for SSA-doped PANI. The power factor decrease continuously within the temperature range with a maximum value 0.94476 $\mu W\ m^{-1}\ K^{-2}$ at room temperature. This value is more than the value (0.0622 $\mu W\ m^{-1}\ K^{-2}$) for the sample doped with bismuth nitrate.[20]

Thermal Conductivity (κ) and Figure of Merit (ZT). The thermal conductivity (κ) and figure of merit (ZT) of SSA and $Bi(NO_3)_3$ doped PANI at room temperature are shown in Figure 4(b). The κ values of SSA and $Bi(NO_3)_3$ doped PANI are found to be 0.1869 and 0.7130 $W\ m^{-1}\ K^{-1}$, respectively, which are very low as compared to the inorganic TE materials. The low value of κ has been originated from the amorphous character of PANI and hence advantageous for TE applications. The ZT values at room temperature of SSA-doped PANI (1.399×10^{-3}) is comparable to that of camphor sulfonic acid doped PANI[7] and for $Bi(NO_3)_3$ doped PANI (2.691×10^{-5}) it is of the order of HCl doped PANI.[31] Thus SSA is a more effective dopant than $Bi(NO_3)_3$ to change the insulating emeraldine base to conducting emeraldine salt. All the transport parameters at room temperature for sample doped with organic and inorganic dopants are tabulated in Table I.

DOPING MECHANISM

As has been proposed by Macdiarmid and co-workers,[36] EB is converted to conducting emeraldine salt (ES) by the process of protonation. Consequently, polarons are formed by the transformation of quinoid to benzoid ring. In EB, the delocalization energy of the π-electron facilitates the C_6 rings to be coplanar. But at the same time, due to the presence of steric interaction,[37] a torsional angle appears[38] as shown in Figure 5(a). The four nitrogen atoms are almost coplanar forming tilt angles with the C_6 rings (from left to right) of 21.0, -39.0, 10.5, and -37.2 respectively.[38] When the EB is protonated to form ES, two of the torsional angles are reduced[38] suggesting a greater conjugation and is attributed to an increase in electrical conductivity.[38]

The doping mechanism of SSA-doped PANI is schematically shown in Figure 5(b). Here single proton dopes the protonation sites of PANI due to which the torsional angle reduces suggesting a greater conjugation and hence we observe a high value of electrical conductivity.

The doping mechanism of bismuth nitrate doped PANI is shown in Figure 5(c). In case of bismuth nitrate [$Bi(NO_3)_3$] doped PANI, two Bi^{3+} ions create bonds with six nitrogen ion of three polyaniline chains as shown in Figure 5(c). Consequently, there is a multiple doping effect which may induce a distortion in the chain of PANI. Thus we observe a higher ordering of chain in case of SSA-doped PANI than $Bi(NO_3)_3$ doped PANI. This is the probable reason for low value of electrical conductivity and thermoelectric power for $Bi(NO_3)_3$ doped PANI than SSA-doped PANI.

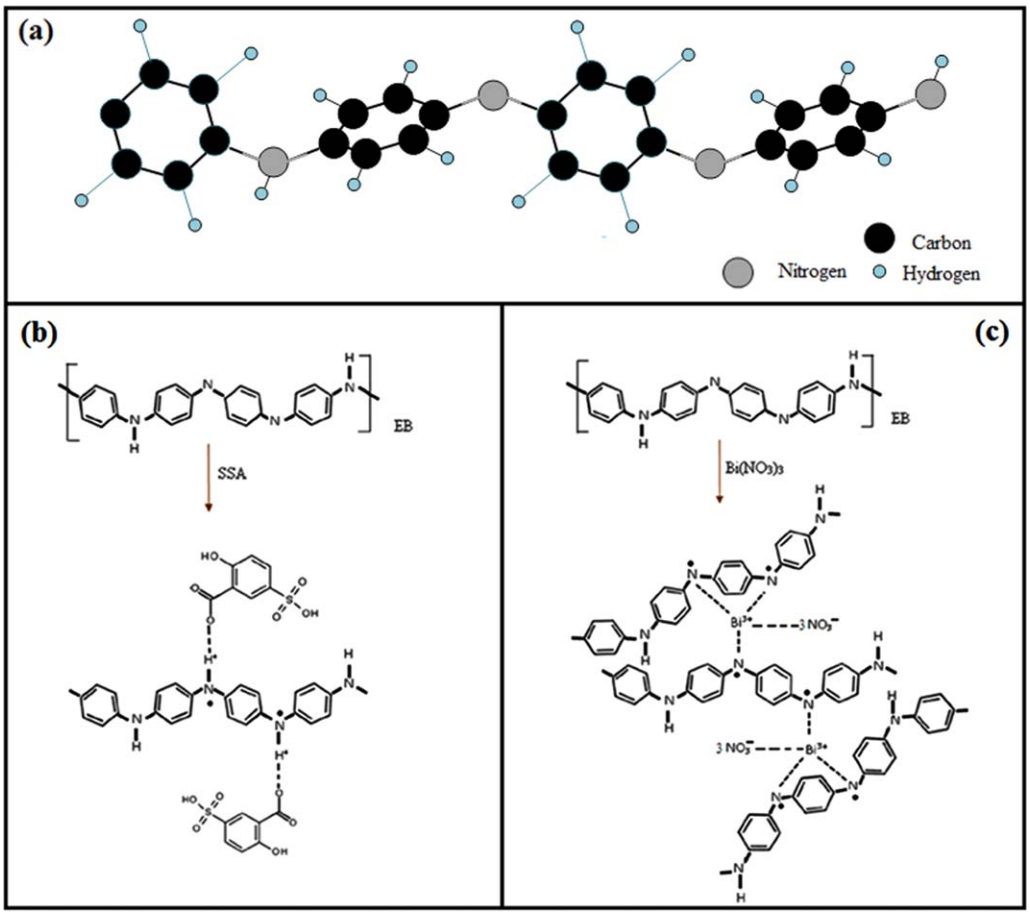

Figure 5. Schematic diagram of (a) structure of polyaniline base (b) doping mechanism of SSA-doped electrodeposited PANI and (c) doping mechanism of $Bi(NO_3)_3$ doped electrodeposited PANI. [Color figure can be viewed in the online issue, which is available at wileyonlinelibrary.com.]

CONCLUSION

An electrochemical deposition was carried out to synthesize PANI doped with SSA.

- The peaks in the FTIR spectrum corresponds to the characteristics bands of PANI. Transmission electron microscopy images reveal that there is formation of long nanorods structure with length and diameter (in nm) 350 and 50 for SSA-doped electrodeposited PANI.
- The electrical conductivity σ is found to change with the type of dopant and increased by five times using organic dopant. Further, temperature variation of σ shows a nonlinearity indicating a metallic type of conduction with hopping or tunneling effects.
- It is observed that electrons are the majority carriers at room temperature confirmed from the negative sign of *S*.
- A proposed equation indicating a hopping mechanism is well fitted with the observed experimental values.
- A comparison of power factor of SSA-doped PANI with the bismuth nitrate doped PANI reveals that power factor is higher for the sample doped with organic dopant at and near room temperatures (300–330 K) than the sample doped with inorganic dopant. The thermal conductivity of SSA-doped PANI is less than bismuth nitrate doped PANI. Consequently the figure of merit of SSA-doped PANI is two order more than bismuth nitrate doped PANI making it a better TE material.

ACKNOWLEDGMENTS

The authors gratefully acknowledge the Department of Science and Technology, India, for financial support and UGC-DAE CSR, Kolkata for using various facilities to carry out the research work. The authors Krishanu Chatterjee and Mousumi Mitra acknowledge CSIR and DST-INSPIRE respectively for financial support.

REFERENCES

1. Feldman, B. J.; Burgmayer, P.; Marray, R. W. *J. Am. Chem. Soc.* **1985**, *107*, 872.
2. Paul, E. W.; Riccio, A. J.; Wrighton, M. S. *J. Phys. Chem.* **1985**, *89*, 1441.
3. Huang, F.; Wang, H. L.; Feldstein, M.; MacDiarmid, A. G.; Hsieh, B. R.; Epstein, A. J. *Synth. Met.* **1997**, *85*, 1283.
4. Gao, J.; Sansiena, J. M.; Wang, H. L. *Synth. Met.* **2003**, *135*, 809.
5. Yan, H.; Toshima, N. *Chem. Lett.* **1999**, *28*, 1217.

6. Shinohara, Y.; Ohara, K.; Imai, Y.; Isoda, Y.; Nakanishi, H. 22nd International Conference on Thermoelectrics IEEE **2003**, pp 298–300.
7. Yan, H.; Sada, N.; Toshima, N. *J. Therm. Anal. Calorim.* **2002**, *69*, 881.
8. Epstein, A. J.; Ginder, J. M.; Zuo, F.; Bigelow, R. W.; Woo, H. S.; Tanner, D. B.; Ritcher, A. F.; Huang, W. H.; Macdiarmid, A. G. *Synth. Met.* **1987**, *18*, 303.
9. Yakuphanoglu, F.; Şenkal, B. F.; Saraç, J. *Electron. Mater.* **2008**, *37*, 930.
10. Ameen, S.; Ali, V.; Zulfequar, M.; Haq, M. M.; Husain, M. *Curr. Appl. Phys.* **2007**, *7*, 215.
11. Long, Y.; Chen, Z. N.; Wang, N.; Zhang, Z.; Wan, M. *Physica B* **2003**, *325*, 208.
12. Song, R. Y.; Park, J. H.; Sivakkumar, S. R.; Kim, S. H.; Ko, J. M.; Rark, D. Y.; Jo, S. M.; Kim, D. Y. *J. Power Sources* **2007**, *166*, 297.
13. Li, H. L.; Wang, J. X.; Chu, Q. X.; Wang, Z.; Zhang, F. B.; Wang, S. C. *J. Power Sources* **2009**, *190*, 578.
14. Mardić, Z.; Roković, M. K. *Electrochim. Acta* **2009**, *54*, 2941.
15. Angelopoulos, M.; Patel, N.; Saraf, R. *Synth. Met.* **1993**, *55*, 1552.
16. Chen, S. A.; Fang, Y.; Lee, H. T. *Synth. Met.* **1993**, *57*, 4082.
17. Tsutsumi, H. *Synth. Met.* **1995**, *69*, 143.
18. Chatterjee, K.; Mitra, M.; Kargupta, K.; Ganguly, S.; Banerjee, D. *Nanotechnology* **2013**, *24*, 215703.
19. Ding, H.; Zhou, G.; Zhu, Y.; Zhang, Y.; Feng, L. *Scripta Mater.* **2013**, *68*, 957.
20. Chatterjee, K.; Ganguly, S.; Kargupta, K.; Banerjee, D. *Synth. Met.* **2011**, *161*, 275.
21. Chatterjee, K.; Ganguly, S.; Kargupta, K.; Banerjee, D. *Mater. Charact.* **2009**, *60*, 1597.
22. Sapurina, I.; Osadchev, A. Y.; Volchek, B. Z.; Trchová, M.; Riede, A.; Stejskal, J. *Synth. Met.* **2002**, *129*, 29.
23. Yan, X. B.; Han, Z. J.; Yang, Y.; Tay, B. T. *Sens. Actuators B.* **2007**, *123*, 107.
24. Athawale, A. A.; Kulkarni, M. V.; Chabukswar, V. V. *Mater. Chem. Phys.* **2002**, *73*, 106.
25. Janošević, A.; Ćirić-Marjanović, G.; Marjanović, B.; Holler, P.; Trchová, M.; Stejskal, J. *Nanotechnology* **2008**, *19*, 135606.
26. Trivedi, D. C.; Dhawan, S. K. *Synth. Met.* **1993**, *58*, 309.
27. Varghese, H. T.; Panicker, C. Y.; Philip, D. *J. Raman Spectrosc.* **2007**, *38*, 309.
28. Tao, S.; Hong, B.; Kerong, Z. *Spectrochim. Acta Part A* **2007**, *66*, 1364.
29. Yang, C.; Chen, C. *Synth. Met.* **2005**, *153*, 133.
30. Lee, K.; Cho, S.; Park, S. H.; Heeger, A. J.; Lee, C. W.; Lee, S. H. *Nature* **2006**, *441*, 65.
31. Li, J.; Tang, X.; Li, H.; Yan, Y.; Zhang, Q. *Synth. Met.* **2010**, *160*, 1153.
32. Kaiser, A. B. *Adv. Mater.* **2001**, *13*, 927.
33. Kaiser, A. B.; Liu, C. J.; Gilberd, P. W.; Chapman, B.; Kemp, N. T.; Wessling, B.; Partridge, A. C.; Smith, W. T.; Shapiro, J. S. *Synth. Met.* **1997**, *84*, 699.
34. Park, Y. W.; Choi, E. S.; Suh, D. S. *Synth. Met.* **1998**, *96*, 81.
35. Holland, E. R.; Pomfert, S. J.; Adams, P. N.; Monkman, A. P. *J. Phys. Condens. Matter* **1996**, *8*, 2991.
36. Stafström, S.; Brédas, J. L.; Epstein, A. J.; Woo, H. S.; Tanner, D. B.; Huang, W. S.; MacDiarmid, A. G. *Phys. Rev. Lett.* **1987**, *59*, 1464.
37. Israelachvili, J. N. *Intermolecular and Surface Forces*; Academic: London, **1985**; Chapter 13, pp 209–210.
38. Álvarez, A. V.; Sordo, J. A.; Scuseria, G. E. *J. Am. Chem. Soc.* **2005**, *127*, 11318.